รายงานเชิงเทคนิค

(TECHNICAL REPORT)

หมายเลขเอกสาร (For OD) **KM Document No.**	SLRI-TR-2024-054
ชื่อเรื่อง **Title**	The effects of asymmetric dipoles for IR sources on SPS-II storage ring
ชื่อฝ่าย **Department**	ฝ่ายปฏิบัติการเครื่องกำเนิดแสงสยาม 1
วันที่เขียนรายงาน **Date of Report**	5 กุมภาพันธ์ 2566
ระดับการเปิดเผยข้อมูล **Level of Disclosure**	☐ ข้อมูลในรายงานเป็นความลับ (Undisclosed)
	☐ เปิดเผยข้อมูลเฉพาะภายในฝ่ายหรือส่วนงาน (Information can be disclosed within department/section)
	☐ เปิดเผยข้อมูลได้สำหรับพนักงานของสถาบันฯ และอนุญาตให้บันทึกข้อมูลเข้าเป็นส่วนหนึ่งของระบบ Knowledge Management ภายในสถาบันฯ (Information can be disclosed for SLRI staffs and can be part of SLRI's Knowledge Management System)
	☑ เปิดเผยข้อมูลได้เพื่อเป็นองค์ความรู้สาธารณะ เช่นเว็บไซต์ของสถาบันฯ (Information is available for public)
คำสำคัญ **Keyword**	Dipole, Light source, IR beamline, Storage ring

รายชื่อผู้ดำเนินโครงการและจัดทำรายงาน **Name**	**ส่วนร่วมในการปฏิบัติงานในโครงการ** **Responsible tasks in the project**
ดร. ฐาปกรณ์ ภู่ลำพงษ์	สร้าง model, ทำการคำนวณ, เขียนรายงาน
ดร. ประไพวรรณ สันวงศ์	ให้ข้อมูล multipole terms

Abstract

Siam Photon Source II (SPS-II) is a new medium size storage ring based light source. SPS-II aims to achieve excellent photon properties and availability. Double-Triple Bend Achromat (DTBA) allows low beam emittance below 1 nm.rad for the ring circumference of about 327 m. It also provides large number of ID beamlines with space in the middle of the cell. The normal dipole field can be utilized to generate IR. Special dipole for IR beamline was designed with larger gap to allow photon extraction. The asymmetric effects emerged from the special dipole with different multipole terms were assessed using frequency map analysis (FMA). No significant difference was found compared with fully symmetry ring with normal dipoles. This suggests that the design can be implemented without major problem.

คำค้น Keyword: Dipole, Light source, IR beamline, Storage ring

1. Introduction

SPS-II is a fourth-generation storage ring designed for low beam emittance utilizing Multi-Bend Achromat (MBA) cell. The lattice for SPS-II [1], Double Triple-Bend Achromat (DTBA), is a modified 6BA providing an additional straight section in the middle of the cell as shown in Figure 1. This doubles the capacity of Insertion Devices (IDs) per unit cell. Noticeably, MBA based design is a compact lattice: narrow space between the magnets. Compactness is unavoidable for the design aiming for maximizing utilization of the machine providing space for sources and instrumentations.

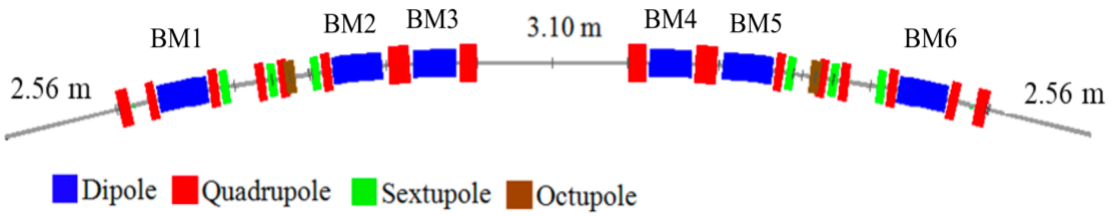

Figure 1 DBA cell lattice design

The main sources of SPS-II are high performance IDs, however; due to the size of SPS-II storage ring is medium whose bending magnet field is up to 0.86 T. This moderate strong field allows possibility for bending magnet to be used as photon source. Thus, bending magnet can be used as IR source.

IR user community is strong in Thailand due to it's application is related to agricultural, medical research which are important. Unlike normal dipole beamline, IR beamline itself has some complications.

Because of the space limit for instrument and photon extraction, bending magnet number 6 (BM6) situated at the end of the DTBA cell as shown in Figure 1 is the most convenient choice. The designated space for IR Beamline must clear the photon extraction condition where the following straight has only diagnostic i.e., DCCT or not occupied by other major source i.e., IDs.

2. Study purpose

2.1 Model the special dipole in SPS-II for IR beamline

2.2 Feasibility study for the IR dipole

2.3 Investigate the effect of a few IR dipole in the SPS-II storage ring on the electron beam

3. Theory/Literature review

In the third generation, storage ring in particular the main sources are insertion devices providing high quality x-rays. While, for infrared (IR), the main sources are bending magnet (BM) constant field emission and edge radiation (ER). To generate and extract IR, bending magnet will be specifically designed. Bending magnet difference can affect linear and non-linear properties of the storage ring.

3.1 Infrared beamlines in low emittance ring

As infrared photons are generated by two main sources: edge radiation (ER), and constant field emission (BM), edge radiation becomes an important source of infrared which should receive increasing interest. [2]

The applications of IR beamlines are quite diverse and impactful. For material Science, IR can be used to analyze material properties, such as composition, crystal structure, and electronic behavior, for the development of new materials or improving existing ones. For Biology and Biomedicine, IR can study biological molecules, proteins, DNA, and cells to understand their structures, functions, and interactions, aiding drug discovery and biomedical research. It can be used for chemical Analysis, Identifying and characterizing chemical compounds, studying reaction kinetics, and understanding molecular dynamics. IR also helps environmental Science for Investigating pollutants, understanding atmospheric chemistry, and analyzing geological samples.

IR beamlines enable researchers to probe matter at a molecular level, providing detailed information that often cannot be obtained through other analytical methods. These facilities are crucial for advancing scientific knowledge and technological developments across various fields.

Bending magnet or dipole is the main component of storage ring controlling the beam path on a designed trajectory. The radiation intensity from dipole as a function of frequency *P*($\boldsymbol{\nu}$) considering long wavelength assuming full integration over vertical angle can be written as

$$\frac{dP(v)}{dv} = 8.64 \times 10^{-7} i\theta(\rho v)^{1/3}$$

Where *i* is the beam current, $\boldsymbol{\theta}$ is the horizontal angular collection in radians and $\boldsymbol{\rho}$ is the bending radius in cm. In modern light sources, beam current is normally high 300-500 mA.

For accelerator magnets, the magnetic field can be described by the expansion with higher order terms

$$\left(B_x - iB_y\right) = i[\sum_n \frac{n \times (A_n + iB_n)}{r \times \left(\frac{z}{r}\right)^{n-1}}]$$

where n is the harmonic order, r is the reference radius. Field errors, in practice, is unavoidable. Systematic field error can emerge naturally since magnet design. Random error caused by random imperfection of manufacturing and assembly processes can be realized later. Pole shape is the critical part reflecting the character of the magnet design and manufacturing. Both error types can be modeled from the magnet design programs.

3.2 Linear effects

The basic parameters that can be affected by different dipole type is linear optics. Quadrupole term introduced by IR dipole need to be corrected using nearby quadrupoles. This allow minimum beta beating and the betatron tune or working point to be preserved. Betatron tune as a function of beta function can be express as

$$\upsilon_{x,y} = \frac{\mu_{x,y}}{2\pi} = \frac{1}{2\pi} \oint \frac{\mathrm{d}u}{\beta_{x,y}(u)},$$

Where $\mu_{x,y}$ is phase advance of the whole ring. Focusing effect from quadrupole can alter betatron function and tune.

3.3 Non-linear effects

In the ideal case, which two different dipole types are made identical for the main field component, the remain higher order terms are still unequal. Quadrupole term and sextupole term can affect chromaticity. Chromaticity or detuning with momentum (p) can be changed according to quadrupole strength (*k*) as follow

$$\xi_{x,y} = \frac{\Delta v_{x,y}}{\Delta p/p_0} = -\frac{1}{4\pi}\oint \beta_{x,y}(s)k_{x,y}(s)\mathrm{d}s\,.$$

This, sometime, is mentioned as natural chromaticity without any correction. It emerges solely from focusing error for off-momentum particles. Thus with different quadrupole term the natural chromaticity will be changed. To correct chromaticity, sextupole term can be included.

$$\xi_x = -\frac{1}{4\pi}\oint \beta_x(s)\cdot[k(s) - m(s)\eta(s)]\mathrm{d}s\,,$$

$$\xi_y = -\frac{1}{4\pi}\oint \beta_y(s)\cdot[k(s) + m(s)\eta(s)]\mathrm{d}s\,.$$

Where *m* is sextupole strength and η is dispersion function. As a consequence, with different quadrupole and sextupole terms, not only the tune needs to be corrected, but chromaticity requires also adjustment.

Moreover, higher order terms driving higher order detuning, resonances and lifetime may be different for the standard and IR dipoles. The terms can be described in the appendix A of this report. This will be assessed using particle tracking after proper parameters correction if required.

4. Methodology / Research design

The study was designed to answer the question of what is the effect of two IR beamline dipole magnets in the SPS-II storage ring? The difference of IR and normal dipole may introduce

asymmetry to the storage ring and associated with worsening storage ring's properties. Basically, the study was divided into two main steps: 1) multipole error extraction 2) particles tracking.

4.1 Multipole terms extraction

From the required wide angle of the IR beam line, hence, the IR dipole magnet need a larger gap than that of the normal dipole. The special dipole for IR beamline clearing the larger gap was designed to have larger iron yoke to support the wider gap. The larger dipole gap, the stronger excitation current is required. Fortunately, the extend vertical size of the yoke allows more space for coils which boosts the ampere turn of the IR dipole and ease the required current.

Magnet design programs have their own style for higher order terms extraction and value. Normally Poisson [3] can be used for 2D design initially and Opera [4] can be used to verify the result for both 2 and 3D design. Multipole terms can be extracted using Fourier series method provided in Opera. Fourier component can be described by

$$F(x) = a_0 + a_1 \cos(2\pi xt) + a_2 \cos(4\pi xt) + \cdots \\ + b_1 \sin(2\pi xt) + b_2 \sin(4\pi xt) + \cdots,$$

where a_n and b_n are normal and skew harmonic terms. Then the harmonic terms can be extracted from the 3D models.

4.2 Particles tracking

Particles tracking is employed as a main tool for this study. To see the effect of multipole terms of the dipoles, frequency map analysis was discussed. Elegant [5] is the main particle tracking code used in this study. Elegant is a mature tracking code and used worldwide by accelerator physicists due to its rich tools and methods.

Higher order field component in dipole can be conveniently implemented in the dipole element. Elegant allows higher order component to be used as k_n (n=1-8) described by the field expansion:

$$B_y(x) = B_0 \times (1 + \sum_{n=1}^{8} \frac{k_n \rho_0}{n!\, x^n})$$

Accelerator element used for dipole is CSBEND : A canonical kick sector dipole magnet. CSBEND is normally used for symplectic tracking and allows upto the eighth order of multipole term expansion. The definition of parameters for CSBEND element is described in Table 1

Table 1 CSBEND element parameters

Parameter Name	Units	Type	Default	Description
L	*M*	double	0.0	arc length
ANGLE	*RAD*	double	0.0	bend angle
K1	$1/M^2$	double	0.0	geometric quadrupole strength
K2	$1/M^3$	double	0.0	geometric sextupole strength
K3	$1/M^4$	double	0.0	geometric octupole strength
K4	$1/M^5$	double	0.0	geometric decapole strength
K5	$1/M^6$	double	0.0	geometric 12-pole strength
K6	$1/M^7$	double	0.0	geometric 14-pole strength
K7	$1/M^8$	double	0.0	geometric 16-pole strength
K8	$1/M^9$	double	0.0	geometric 18-pole strength
E1	*RAD*	double	0.0	entrance edge angle
E2	*RAD*	double	0.0	exit edge angle
TILT	*RAD*	double	0.0	rotation about incoming longitudinal axis
H1	$1/M$	double	0.0	entrance pole-face curvature
H2	$1/M$	double	0.0	exit pole-face curvature
HGAP	*M*	double	0.0	half-gap between poles
FINT		double	0.5	edge-field integral
FINT1		double	-1	edge-field integral. If negative, use FINT.
FINT2		double	-1	edge-field integral. If negative, use FINT.
DX	*M*	double	0.0	misalignment
DY	*M*	double	0.0	misalignment
DZ	*M*	double	0.0	misalignment
XKICK	*RAD*	double	0.0	bend-plane steering angle (approximate)
YKICK	*RAD*	double	0.0	non-bend-plane steering angle (approximate)
FSE		double	0.0	fractional strength error of all components
FSE_DIPOLE		double	0.0	fractional strength error of dipole component

From the element parameters in Table 1, it is quite simple to define the higher order field component. Geometric strength for order n can be written as k_n. which can be implemented in the lattice file which all the parameters of each element can be defined, and the machine structure can be built. The maximum multipole term can be defined is 8^{th} or 18-pole geometric term.

After indicating all the multipole terms for each dipole type, particles tracking with Frequency map analysis (FMA) [6] will be employed to determine the effect of the terms. FMA can be done by following steps:

1) Define the total number of turn (N) for particle tracking
2) Define the tracking boundary on x-y or δ_P-x plane
3) Define the number of point on the boundary (grid size) depends on how much detail required
4) Split the total number of turns into half N/2
5) For each surviving grid point
   Do a particle tracking for the first N/2
   Then do another half of N/2 turns tracking
   Calculate tune ($\boldsymbol{\nu}$) for both first and second step tracking on both plane x-y or x-dp
   Calculate diffusion rate d_r:

$$d_r = \log_{10}\left(\frac{\sqrt{\Delta\nu_x^2 + \Delta\nu_y^2}}{N}\right)$$

6) Plot the grid point with color coded based on the diffusion rate
7) Plot all the points in the tune space to see the tune map

Based on the calculated diffusion rate, $\boldsymbol{\Delta\nu}$ determines the tune different between two tracking steps indicating the tune stability of each point. If the diffusion rate is low the tracked particle is more likely to survive for many turns. As a consequence, it is a convenient way to assess the stability track the evolution of each point in the tune space.

5 Results and Discussion

In this section, results of dipole magnets design, higher order magnetic field terms and their effect on the electron beam dynamics in the SPS-II storage ring will be discussed.

The required bending angle was used for dipole design. It should provide correct bending angle for electron beam around the storage ring. Magnet designers then design the dipoles from the angle which reflects on the field strength and magnetic gap. Ideally to minimize the exciting current for EM magnet, the gap should be as small as possible. However, the minimum gap will be constraint by the beam stay clear and vacuum components for the storage ring. For SPS-II Dipole design [7] for both normal and IR beamline will be different as shown in Figure 2. The gap of dipole for IR beamline needs to be large enough for IR extraction. The gap of 59 mm is then required for IR beamline instead of standard 36 mm. Larger dipole gap needs stronger excitation current as compared in Figure 3. To reach the operating field of 0.87 T, the IR dipole needs above 21,000 A.turns while the standard one requires lower than 13,000 A.turns.

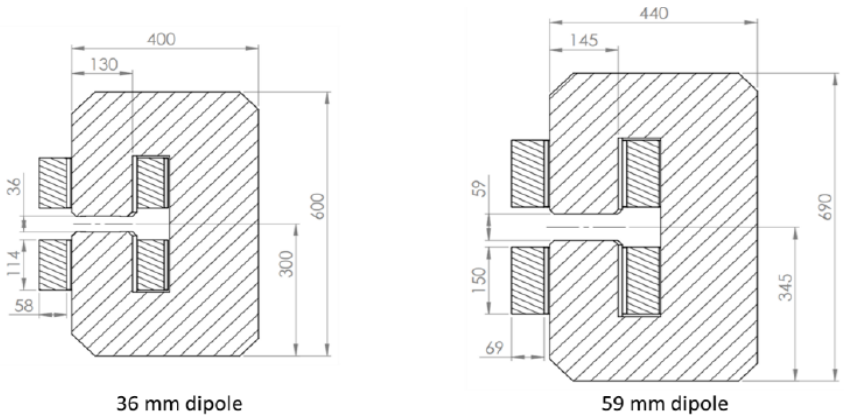

Figure 2 Cross section of normal dipole (left) and IR beamline dipole (right) for SPS-II

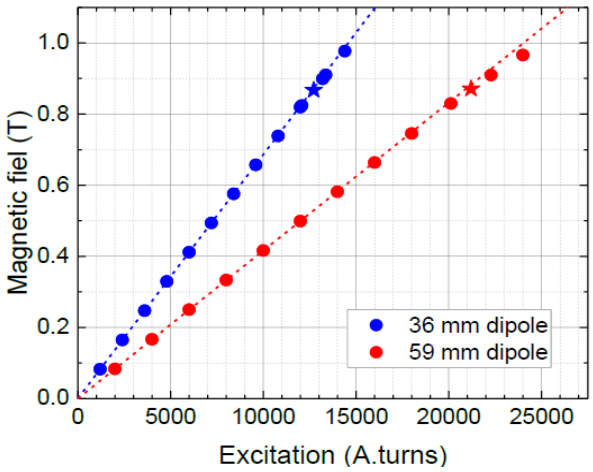

Figure 3 Magnetic field as a function of excitation current for 36mm and 59mm gap dipoles

5.1 **Higher order terms for Dipoles**

The extracted multipole field for normal and IR beamline dipoles are summarized in Table 2 and Table 3 respectively.

Table 2 Higher order field for normal dipole

n	nBn/R (T/mm)	Bn	Norm Bn	nAn/R (T/mm)	An	Norm An
1	-8.71E+02	-1.04E+04	1.00E+00	0.00E+00	0.00E+00	0.00E+00
2	7.80E-02	4.68E-01	-4.48E-05	-2.48E-10	-1.49E-09	1.42E-13
3	7.61E-01	3.04E+00	-2.91E-04	5.27E-12	2.11E-11	-2.02E-15
4	-4.82E-02	-1.45E-01	1.38E-05	-1.00E-09	-3.01E-09	2.89E-13
5	-3.23E-02	-7.76E-02	7.43E-06	1.50E-12	3.59E-12	-3.44E-16
6	-3.06E-03	-6.11E-03	5.85E-07	9.63E-10	1.93E-09	-1.84E-13
7	-7.57E-03	-1.30E-02	1.24E-06	-3.89E-12	-6.67E-12	6.38E-16
8	-4.40E-03	-6.60E-03	6.32E-07	3.55E-10	5.33E-10	-5.10E-14
9	-8.84E-04	-1.18E-03	1.13E-07	-3.02E-12	-4.02E-12	3.85E-16
10	6.98E-04	8.38E-04	-8.02E-08	-6.21E-10	-7.45E-10	7.13E-14
11	-9.12E-04	-9.95E-04	9.53E-08	2.32E-12	2.54E-12	-2.43E-16
12	-2.19E-03	-2.19E-03	2.10E-07	-1.52E-10	-1.52E-10	1.45E-14
13	8.54E-04	7.88E-04	-7.54E-08	2.79E-12	2.58E-12	-2.47E-16
14	-8.32E-04	-7.13E-04	6.83E-08	-1.24E-11	-1.06E-11	1.01E-15

Table 3 Higher order field for IR beamline dipole

n	nBn/R (T/mm)	Bn	Norm Bn	nAn/R (T/mm)	An	Norm An
1	-8.71E+02	-1.05E+04	1.00E+00	0.00E+00	0.00E+00	0.00E+00
2	1.03E-01	6.18E-01	-5.91E-05	-2.46E-10	-1.47E-09	1.41E-13
3	4.96E-01	1.98E+00	-1.90E-04	5.05E-12	2.02E-11	-1.93E-15
4	-5.59E-02	-1.68E-01	1.60E-05	-9.95E-10	-2.98E-09	2.85E-13
5	-1.98E-02	-4.75E-02	4.55E-06	1.60E-12	3.85E-12	-3.68E-16
6	-5.76E-03	-1.15E-02	1.10E-06	9.53E-10	1.91E-09	-1.82E-13
7	5.10E-04	8.74E-04	-8.36E-08	-3.90E-12	-6.69E-12	6.40E-16
8	1.18E-03	1.77E-03	-1.69E-07	3.52E-10	5.28E-10	-5.05E-14
9	-1.57E-03	-2.09E-03	2.00E-07	-2.97E-12	-3.96E-12	3.78E-16
10	-1.04E-04	-1.25E-04	1.19E-08	-6.15E-10	-7.38E-10	7.06E-14
11	1.60E-03	1.75E-03	-1.67E-07	2.13E-12	2.33E-12	-2.23E-16
12	-1.90E-03	-1.90E-03	1.82E-07	-1.50E-10	-1.50E-10	1.44E-14
13	-1.09E-03	-1.01E-03	9.66E-08	2.83E-12	2.61E-12	-2.50E-16
14	5.97E-04	5.12E-04	-4.89E-08	-1.22E-11	-1.05E-11	1.00E-15

The values in Table 2 and Table 3 are not immediately useable in the model. For Elegant, strength will be accepted in the model. The strength for each order can be computed conveniently as

$$k_n = \frac{n!}{B_0\rho_0}\frac{B_n}{r_0^n}$$

Where n is the Lego order, which n=0 for dipole component, $B_0\boldsymbol{\rho}_0$ is the magnet rigidity (3.3356 x E = 10.0068 T.m) where E is the beam energy of 3 GeV for SPS-II.

As a result, conversion can be made with the above equation providing strength to be used in the model as listed in Table 4.

Table 4 Higher order geometric strength for normal (left) and IR beamline (right) dipoles

order	kn (1/m^n)	
	Normal	Skew
1	6.4936E-04	-2.0633E-12
2	1.0562E+00	7.3171E-12
3	-1.6723E+01	-3.4869E-07
4	-3.7405E+03	1.7313E-07
5	-1.4731E+05	4.6391E-02
6	-1.8229E+08	-9.3697E-02
7	-6.1834E+10	4.9913E+03
8	-8.2829E+12	-2.8276E+04
9	4.9063E+15	-4.3645E+09
10	-5.3437E+18	1.3615E+10
11	-1.1771E+22	-8.1416E+14
12	4.5837E+24	1.4992E+16
13	-4.8402E+27	-7.1955E+19

order	kn (1/m^n)	
	Normal	Skew
1	8.5724E-04	-2.0450E-12
2	6.8824E-01	7.0053E-12
3	-1.9407E+01	-3.4523E-07
4	-2.2904E+03	1.8546E-07
5	-2.7735E+05	4.5931E-02
6	1.2282E+07	-9.4039E-02
7	1.6603E+10	4.9457E+03
8	-1.4714E+13	-2.7810E+04
9	-7.3162E+14	-4.3209E+09
10	9.3829E+18	1.2491E+10
11	-1.0226E+22	-8.0668E+14
12	-5.8756E+24	1.5182E+16
13	3.4719E+27	-7.1232E+19

The maximum order accepted by CSBEND in Elegant is 8^{th}. Thus, from the calculated geometric strength, normal dipole element definition in Elegant lattice file can be written as

```
DL1E: CSBEND,L=1,ANGLE=0.08671706584501949,E1=0.04335853292250975,&
 E2=0.04335853292250975,N_KICKS=40,SYNCH_RAD=1,&
 K1=6.4936E-04,&
 K2=1.0562E+00,&
 K3=-1.6723E+01,&
 K4=-3.7405E+03,&
 K5=-1.4731E+05,&
 K6=-1.8229E+08,&
 K7=-6.1834E+10,&
 K8=-8.2829E+12
```

Similarly, the dipole for IR beamline can be written as

```
DLIR: CSBEND,L=1,ANGLE=0.08671706584501949,E1=0.04335853292250975,&
 E2=0.04335853292250975,N_KICKS=40,SYNCH_RAD=1,&
 K1=8.5724E-04,&
 K2=6.8824E-01,&
 K3=-1.9407E+01,&
 K4=-2.2904E+03,&
 K5=-2.7735E+05,&
 K6=1.2282E+07,&
 K7=1.6603E+10,&
 K8=-1.4714E+13
```

Observably, quadrupole term for IR beamline dipole is stronger than that of the normal dipole. While sextupole term is larger in normal dipole. Most of the other terms are in the similar order.

5.2 Effects on the storage ring

As the higher order terms were modeled, particles tracking results for different conditions are shown by FMA x-y in Figure 4-Figure 6. The effect on the transverse plane can be compared.

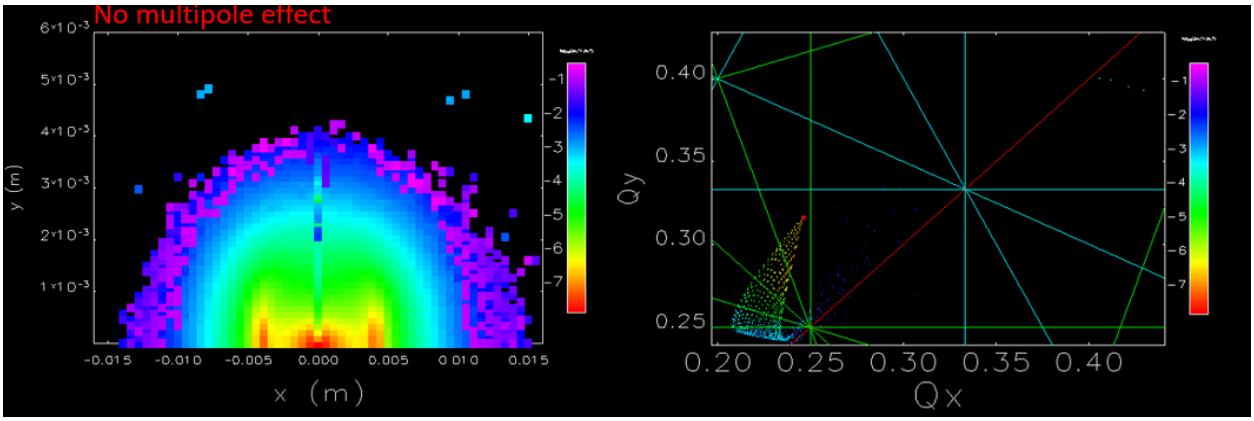

Figure 4 FMA x-y without any multipole error

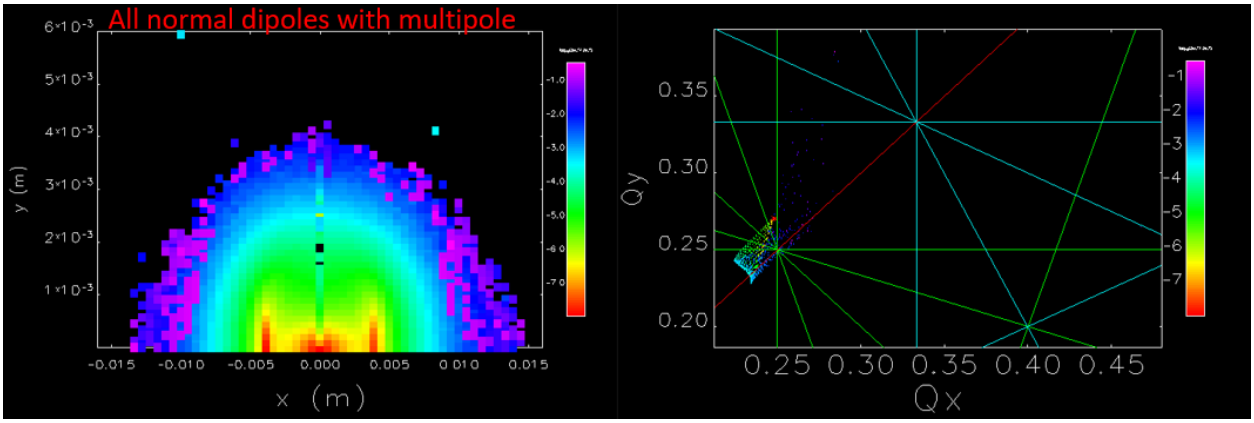

Figure 5 FMA x-y with multipole error in all normal dipoles

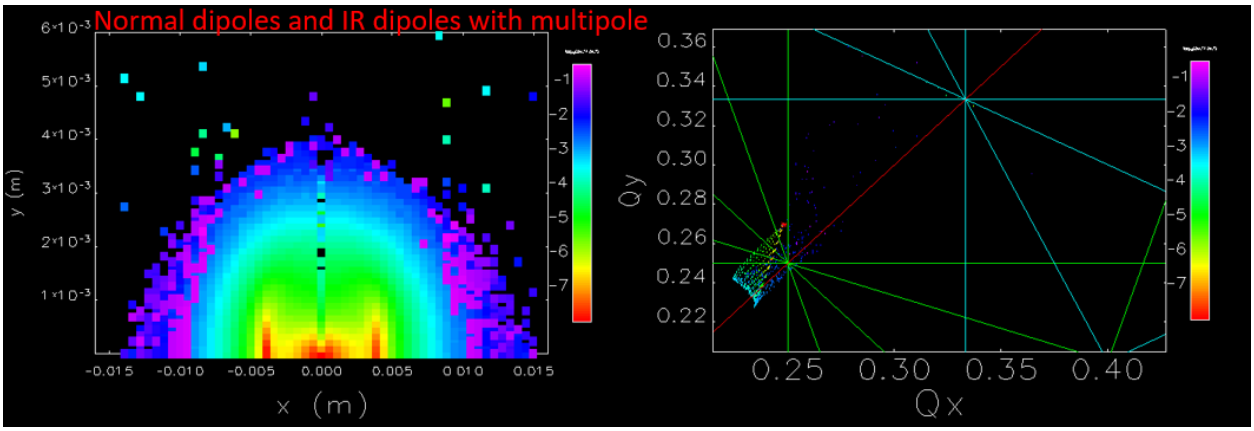

Figure 6 FMA x-y with multipole error in all normal and IR dipoles

Similarly, particles tracking results for different conditions are shown by FMA δ_P-x in Figure 7-Figure 9. Then the effect on the longitudinal plane can be compared.

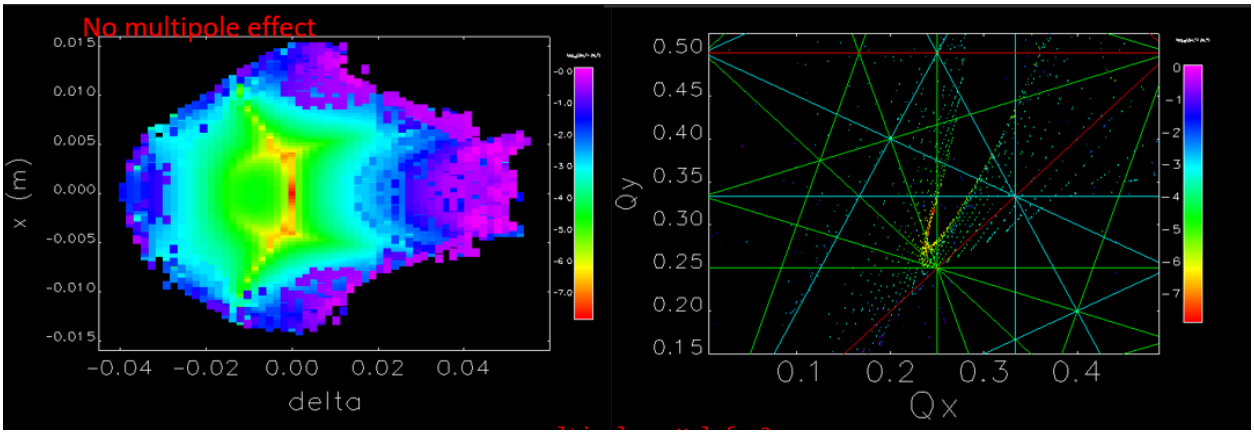

Figure 7 FMA δ_P-x without any multipole error

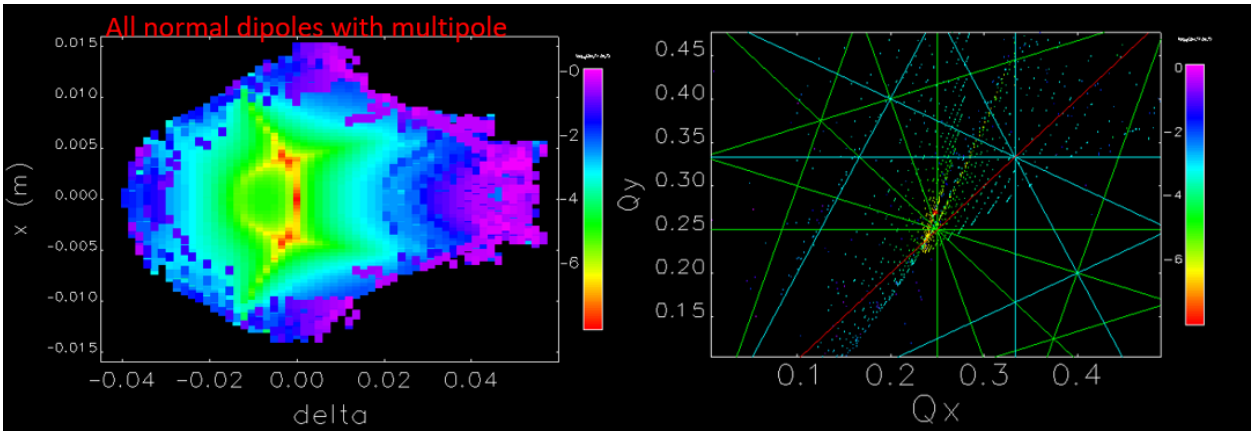

Figure 8 FMA δ_P-x with multipole error in all normal dipoles

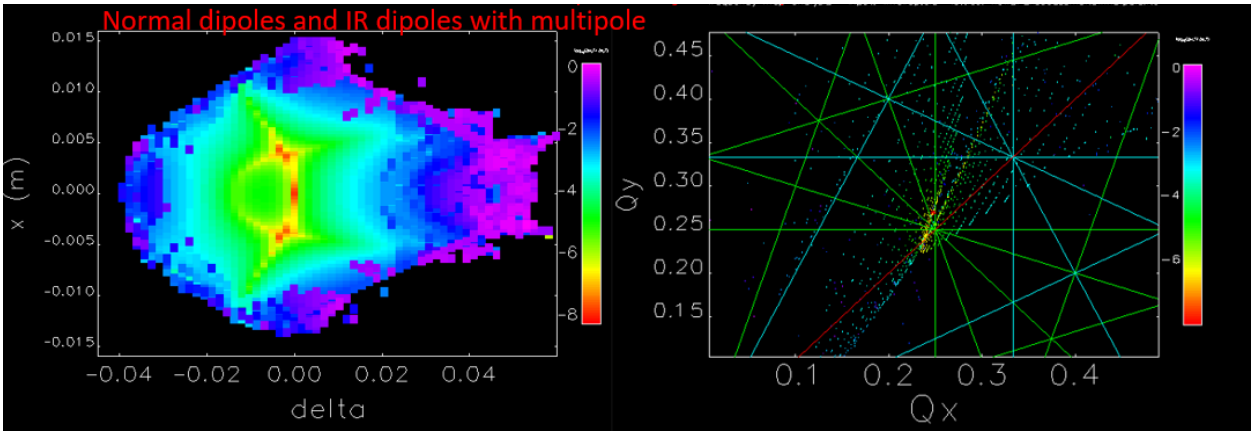

Figure 9 FMA δ_P-x with multipole error in all normal and IR dipoles

Three conditions of particle tracking: Ideal machine without multipole error, machine with only normal dipoles with multipole error and machine with normal and IR dipoles with multipole error were discussed. From the FMA results, there is no noticeable difference for both x-y and δ_p-x planes.

6. Conclusion

FMA for x-y and δ_p-x were investigated with particle tracking in Elegant. These should allow good evaluation of the dipole effect on the transverse and longitudinal planes. Multipole terms from normal and IR dipoles were included. The simulated results show unnoticeable effect between the multipole terms from normal dipoles and IR dipole. This due to only few IR dipoles in the ring compared to 84 normal dipoles. Negligible effect on the electron dynamic suggests that the IR dipoles can be applied to SPS-II storage ring.

Though the feasibility of IR dipole is confirmed, budget and time limit may not allow the IR beamline to be built in the first phase. SPS-II has prepared the feasibility study and design to be ready in the future.

7. Users

- Particle accelerator physicists can use the results to evaluate a proper working solution for IR beamline design.
- Magnet designer
- Magnet manufacturer
- Beamline designer

References

[1] P. Klysubun, T. Pulampong and P. Sudmuang, "Design and Optimisation of SPS-II Storage Ring," in *Proceedings of IPAC2017*, Copenhagen, Denmark, 2017.

[2] P. Dumas, "Synchrotron Infrared Beamlines at Ultra-Low Emittance Facilities: challenges and perspectives".

[3] M. T. Menzel and H. K. Stokes, "User's Guide for the POISSON/SUPERFISH Group of Codes," Los Alamos, 1987.

[4] Vector Field Limited, "OPERA-3D USER GUIDE," Oxford, 2004.

[5] M. Borland, "elegant: A Flexible SDDS-Compliant Code for Accelerator Simulation," Advanced Photon Source, 2000.

[6] J. Laskar, "Frequency map analysis and particle accelerators," in *Particle Accelerator Conference*, 2003.

[7] P. Sunwong, "Design of dipole magnets for Siam Photon Source II," in *Journal of Physics: Conference Series*, 2023.

ภาคผนวก

Higher order driving terms

Analytic formulae

A.1 Resonance driving terms formulas

Resonance driving terms (RDTs) were derived in the early works [43] and [94]. Each driving term drives different phenomenon or resonance of particles. The driving term h_{abcde} whose subscript indicates what resonance effect can be excited by the term. Generally, the driving term indicates the resonance

$$(a-b)\nu_x + (c-d)\nu_y = n \tag{A.1}$$

where n is an integer number. The index e is related to dispersion or chromatic terms. The resonance driving term can be written explicitly in term of optics functions ($\beta_{x,y}$, η_x) and quadrupole and sextupole integrated strength (b_2 and b_3) as follows.

A.1.1 First order chromatic driving terms

$$h_{11001} = \frac{1}{4}\sum_{i=1}^{N}\big[(b_2L)_i - 2(b_3L)\eta_{xi}\big]\beta_{xi} + O(\delta^2), \tag{A.2}$$

$$h_{00111} = -\frac{1}{4}\sum_{i=1}^{N}\big[(b_2L)_i - 2(b_3L)\eta_{xi}\big]\beta_{yi} + O(\delta^2), \tag{A.3}$$

$$h_{20001} = \frac{1}{8}\sum_{i=1}^{N}\big[(b_2L)_i - 2(b_3L)_i\eta_{xi}\big]\beta_{xi}e^{i2\mu_{xi}} + O(\delta^2) \tag{A.4}$$

$$h_{00201} = -\frac{1}{8}\sum_{i=1}^{N}\big[(b_2L)_i - 2(b_3L)_i\eta_{xi}\big]\beta_{yi}e^{i2\mu_{yi}} + O(\delta^2) \tag{A.5}$$

$$h_{10002} = \frac{1}{2}\sum_{i=1}^{N}\big[(b_2L)_i - (b_3L)_i\eta_{xi}\big]\eta_{xi}^{(1)}\sqrt{\beta_{xi}}e^{i2\mu_{xi}} + O(\delta^3) \tag{A.6}$$

In the chromatic terms, the effects of sextupoles can be used to counteract the effects generated by quadrupole after linear optics matching. h_{11001} and h_{00111} drives chromaticities in horizontal and vertical plane respectively. Chromatic sextupole can control the term effectively in non-dispersive sections. Normally, dispersion bumps are intentionally generated at the position of chromatic sextupoles to ease the correction.

A.1.2 First order geometric driving terms

$$h_{21000} = -\frac{1}{8}\sum_{i=1}^{N}(b_{3i}L)\beta_{xi}^{\frac{3}{2}}e^{i\mu_{xi}}, \tag{A.7}$$

$$h_{30000} = -\frac{1}{24}\sum_{i=1}^{N}(b_{3i}L)\beta_{xi}^{\frac{3}{2}}e^{i3\mu_{xi}}, \tag{A.8}$$

$$h_{10110} = \frac{1}{4}\sum_{i=1}^{N}(b_{3i}L)\beta_{xi}^{\frac{1}{2}}\beta_{yi}e^{i\mu_{xi}}, \tag{A.9}$$

$$h_{10020} = \frac{1}{8}\sum_{i=1}^{N}(b_{3i}L)\beta_{xi}^{\frac{1}{2}}\beta_{yi}e^{i(\mu_{xi}-2\mu_{yi})}, \tag{A.10}$$

$$h_{10200} = \frac{1}{8}\sum_{i=1}^{N}(b_{3i}L)\beta_{xi}^{\frac{1}{2}}\beta_{yi}e^{i(\mu_{xi}+2\mu_{yi})} \tag{A.11}$$

The geometric driving terms are contributed by sextupole magnets in the ring. Although the sextupoles are used to control the chromatic term especially chromaticities, they also introduce geometric terms. To suppress these term, harmonic sextupoles can be introduced in straight section where dispersion function is small to avoid the increase of the chromatic terms.

A.1.3 Second order driving terms

For second order driving terms, the explicit formulae can be found in [94]. When sextupoles are introduced into a lattice high order resonance can be excited. The strengths of the driving terms increase with stronger sextupole strength.

The summation appears in the following formulae is defined as

$$\sum f(i,j) \equiv \sum_{j>i}\big[f(i,j)-f(j,i)\big] = \sum_{j=1}^{N}\sum_{i=1}^{j}\big[f(i,j)-f(j,i)\big] = \left(\sum_{j>i}-\sum_{i>j}\right)f(i,j) \tag{A.12}$$

Hence the second order geometric terms can be expressed as follows:

A.1 Resonance driving terms formulas

$$h_{22000} = \sum \frac{i}{64} b_{3i} b_{3j} \beta_{xi}^{3/2} \beta_{xj}^{3/2} \left[e^{i3(\mu_{xi}-\mu_{xj})} + 3e^{i(\mu_{xi}-\mu_{xj})} \right], \tag{A.13}$$

$$h_{31000} = h^*_{13000} = \sum \frac{i}{32} b_{3i} b_{3j} \beta_{xi}^{3/2} \beta_{xj}^{3/2} e^{i(3\mu_{xi}-\mu_{xj})}, \tag{A.14}$$

$$h_{21010} = 0 \tag{A.15}$$

$$h_{21100} = 0 \tag{A.16}$$

$$h_{11110} = \sum \frac{i}{16} b_{3i} b_{3j} \sqrt{\beta_{xi}\beta_{xj}\beta_{yi}} \Big\{ \beta_{xj} \left[e^{-i(\mu_{xi}-\mu_{xj})} - e^{i(\mu_{xi}-\mu_{xj})} \right] + \beta_{yj} \left[e^{i(\mu_{xi}-\mu_{xj}+2\mu_{yi}-2\mu_{yj})} + e^{-i(\mu_{xi}-\mu_{xj}-2\mu_{yi}+2\mu_{yj})} \right] \Big\}, \tag{A.17}$$

$$h_{11200} = \sum \frac{i}{32} b_{3i} b_{3j} \sqrt{\beta_{xi}\beta_{xj}\beta_{yi}} \Big\{ \beta_{xj} \left[e^{-i(\mu_{xi}-\mu_{xj}-2\mu_{yi})} - e^{i(\mu_{xi}-\mu_{xj}+2\mu_{yi})} \right] + 2\beta_{yj} \left[e^{i(\mu_{xi}-\mu_{xj}+2\mu_{yi})} + e^{-i(\mu_{xi}-\mu_{xj}-2\mu_{yi})} \right] \Big\}, \tag{A.18}$$

$$h_{40000} = \sum \frac{i}{64} b_{3i} b_{3j} \beta_{xi}^{3/2} \beta_{xj}^{3/2} e^{i(3\mu_{xi}+\mu_{xj})}, \tag{A.19}$$

$$h_{30010} = 0, \tag{A.20}$$

$$h_{30100} = 0, \tag{A.21}$$

$$h_{20020} = \sum \frac{i}{64} b_{3i} b_{3j} \sqrt{\beta_{xi}\beta_{xj}\beta_{yi}} \left[\beta_{xj} e^{-i(\mu_{xi}-3\mu_{xj}+2\mu_{yi})} \right. \tag{A.22}$$

$$\left. -(\beta_{xj} + 4\beta_{yj}) e^{i(\mu_{xi}+\mu_{xj}-2\mu_{yj})} \right], \tag{A.23}$$

$$h_{20110} = \sum \frac{i}{32} b_{3i} b_{3j} \sqrt{\beta_{xi}\beta_{xj}\beta_{yi}} \Big\{ \beta_{xj} \left[e^{-i(\mu_{xi}-3\mu_{xj})} - e^{i(\mu_{xi}+\mu_{xj})} \right] \tag{A.24}$$

$$+2\beta_{yj} e^{i(\mu_{xi}+\mu_{xj}+2\mu_{yi}-2\mu_{yj})} \Big\}, \tag{A.25}$$

$$h_{20200} = \sum \frac{i}{64} b_{3i} b_{3j} \sqrt{\beta_{xi}\beta_{xj}\beta_{yi}} \left[\beta_{xj} e^{-i(\mu_{xi}-3\mu_{xj}-2\mu_{yi})} \right. \tag{A.26}$$

$$\left. -(\beta_{xj} - 4\beta_{yj}) e^{i(\mu_{xi}+\mu_{xj}+2\mu_{yj})} \right], \tag{A.27}$$

$$h_{10030} = 0, \tag{A.28}$$

$$h_{10120} = 0, \tag{A.29}$$

$$h_{10210} = 0, \tag{A.30}$$

$$h_{10300} = 0, \tag{A.31}$$

$$h_{00220} = \sum \frac{i}{64} b_{3i} b_{3j} \sqrt{\beta_{xi}\beta_{xj}\beta_{yi}\beta_{yj}} \left[e^{i(\mu_{xi}-\mu_{xj}+2\mu_{yi}-2\mu_{yj})} \right. + 4e^{i(\mu_{xi}-\mu_{xj})} - \left. e^{-i(\mu_{xi}-\mu_{xj}-2\mu_{yi}+2\mu_{yj})} \right], \tag{A.32}$$

$$h_{00310} = \sum \frac{i}{32} b_{3i} b_{3j} \sqrt{\beta_{xi}\beta_{xj}\beta_{yi}\beta_{yj}} \left[e^{i(\mu_{xi}-\mu_{xj}+2\mu_{yi})} - e^{-i(\mu_{xi}-\mu_{xj}-2\mu_{yi})} \right], \tag{A.33}$$

$$h_{00400} = \sum \frac{i}{64} b_{3i} b_{3j} \sqrt{\beta_{xi}\beta_{xj}\beta_{yi}\beta_{yj}} e^{i(\mu_{xi}-\mu_{xj}+2\mu_{yi}+2\mu_{yj})}, \tag{A.34}$$

$$h_{21001} = \sum \Big\{ -\frac{i}{32} b_{3i} b_{2j} \beta_{xi}^{3/2} \beta_{xj} \left[e^{i\mu_{xi}} + e^{i(3\mu_{xi}-2\mu_{xj})} - 2e^{-i(\mu_{xi}-2\mu_{xj})} \right] - \frac{i}{16} b_{3i} b_{3j} \beta_{xi} \beta_{xj}^{3/2} \eta_{xi} \left[e^{i\mu_{xj}} - 2e^{i(2\mu_{xi}-\mu_{xj})} + e^{-i(2\mu_{xi}-3\mu_{xj})} \right] \Big\}, \tag{A.35}$$

$$h_{11101} = 0, \tag{A.36}$$

$$h_{30001} = \sum \Big\{ -\frac{i}{32} b_{3i} b_{2j} \beta_{xi}^{3/2} \beta_{xj} \left[e^{i3\mu_{xi}} - e^{i(\mu_{xi}+2\mu_{xj})} \right] - \frac{i}{16} b_{3i} b_{3j} \beta_{xi} \beta_{xj}^{3/2} \eta_{xi} \left[e^{i3\mu_{xj}} - e^{i(2\mu_{xi}+\mu_{xj})} \right] \Big\}, \tag{A.37}$$

A.1 Resonance driving terms formulas

$$h_{20011} = 0, \tag{A.38}$$

$$h_{20101} = 0, \tag{A.39}$$

$$\begin{aligned} h_{10021} = \sum \Big\{ & \frac{i}{32} b_{3i} b_{2j} \sqrt{\beta_{xi}\beta_{xj}\beta_{yi}} \left[e^{i(\mu_{xi}-2\mu_{yi})} - e^{-i(\mu_{xi}-2\mu_{xj}+2\mu_{yi})} \right] \\ & + \frac{i}{16} b_{3i} b_{2j} \sqrt{\beta_{xi}\beta_{yj}\beta_{yi}} \left[e^{i(\mu_{xi}-2\mu_{yi})} - e^{i(\mu_{xi}-2\mu_{yj})} \right] \\ & + \frac{i}{16} b_{3i} b_{3j} \beta_{xi} \sqrt{\beta_{xj}\beta_{yj}\eta_{xi}} \left[e^{i(\mu_{xj}-2\mu_{yj})} - e^{i(2\mu_{xi}-\mu_{xj}-2\mu_{yj})} \right] \\ & - \frac{i}{8} b_{3i} b_{3j} \sqrt{\beta_{xj}\beta_{yj}\beta_{yi}\eta_{xi}} \left[e^{i(\mu_{xj}-2\mu_{yi})} - e^{i(\mu_{xj}-2\mu_{yj})} \right] \Big\}, \end{aligned} \tag{A.40}$$

$$\begin{aligned} h_{10111} = \sum \Big\{ & \frac{i}{16} b_{3i} b_{2j} \sqrt{\beta_{xi}\beta_{xj}\beta_{yi}} \left[e^{i\mu_{xi}} - e^{-i(\mu_{xi}-2\mu_{xj})} \right] \\ & + \frac{i}{16} b_{3i} b_{2j} \sqrt{\beta_{xi}\beta_{yj}\beta_{yi}} \left[e^{i(\mu_{xi}-2\mu_{yi}+2\mu_{yj})} - e^{i(\mu_{xi}+2\mu_{yi}-2\mu_{yj})} \right] \\ & + \frac{i}{8} b_{3i} b_{3j} \beta_{xi} \sqrt{\beta_{xj}\beta_{yj}\eta_{xi}} \left[e^{i\mu_{xj}} - e^{i(2\mu_{xi}-\mu_{xj})} \right] \\ & - \frac{i}{8} b_{3i} b_{3j} \sqrt{\beta_{xj}\beta_{yj}\beta_{yi}\eta_{xi}} \left[e^{i(\mu_{xj}-2\mu_{yi}+2\mu_{yj})} - e^{i(\mu_{xj}+2\mu_{yi}-2\mu_{yj})} \right] \Big\}, \end{aligned} \tag{A.41}$$

$$\begin{aligned} h_{10201} = \sum \Big\{ & \frac{i}{32} b_{3i} b_{2j} \sqrt{\beta_{xi}\beta_{xj}\beta_{yi}} \left[e^{i(\mu_{xi}+2\mu_{yi})} - e^{-i(\mu_{xi}-2\mu_{xj}-2\mu_{yi})} \right] \\ & - \frac{i}{16} b_{3i} b_{2j} \sqrt{\beta_{xi}\beta_{yj}\beta_{yi}} \left[e^{i(\mu_{xi}-2\mu_{yi}+2\mu_{yj})} - e^{i(\mu_{xi}+2\mu_{yi}-2\mu_{yj})} \right] \\ & + \frac{i}{16} b_{3i} b_{3j} \beta_{xi} \sqrt{\beta_{xj}\beta_{yj}\eta_{xi}} \left[e^{i(\mu_{xj}+2\mu_{yj})} - e^{i(2\mu_{xi}-\mu_{xj}+2\mu_{yj})} \right] \\ & + \frac{i}{8} b_{3i} b_{3j} \sqrt{\beta_{xj}\beta_{yj}\beta_{yi}\eta_{xi}} \left[e^{i(\mu_{xj}+2\mu_{yi})} - e^{i(\mu_{xj}+2\mu_{yj})} \right] \Big\}, \end{aligned} \tag{A.42}$$

$$h_{00211} = 0, \tag{A.43}$$

$$h_{00301} = 0, \tag{A.44}$$

$$\begin{aligned} h_{11002} = \sum \Big\{ & \frac{i}{16} \beta_{xi}\beta_{xj} \left[(b_{2i}b_{2j} - 2b_{3i}b_{2j}\eta_{xi} + 4b_{3i}b_{3j}\eta_{xi}\eta_{xj}) e^{i2(\mu_{xi}-\mu_{xj})} + 2b_{3i}b_{2j}\eta_{xi} e^{-i2(\mu_{xi}-\mu_{xj})} \right] \\ & + \frac{i}{8} \sqrt{\beta_{xi}\beta_{xj}^{3/2}} \eta_{xi} (b_{3i}\eta_{xi} - b_{2i}) b_{3j} \left[e^{i(\mu_{xi}-\mu_{xj})} - e^{-i(\mu_{xi}-\mu_{xj})} \right] \Big\}, \end{aligned} \tag{A.45}$$

$$\begin{aligned} h_{20002} = \sum \Big\{ & \frac{i}{16} \beta_{xi}\beta_{xj} \left[(b_{2i}b_{2j} - 2b_{3i}b_{2j}\eta_{xi} + 4b_{3i}b_{3j}\eta_{xi}\eta_{xj}) e^{i2\mu_{xi}} + 2b_{3i}b_{2j}\eta_{xi} e^{i2\mu_{xj}} \right] \\ & + \frac{i}{16} \sqrt{\beta_{xi}\beta_{xj}^{3/2}} \eta_{xi} (b_{3i}\eta_{xi} - b_{2i}) b_{3j} \left[e^{i(\mu_{xi}+\mu_{xj})} - e^{-i(\mu_{xi}-3\mu_{xj})} \right] \Big\}, \end{aligned} \tag{A.46}$$

$$h_{10012} = 0, \tag{A.47}$$

$$h_{10102} = 0, \tag{A.48}$$

$$\begin{aligned} h_{00112} = \sum \Big\{ & \frac{i}{16} \beta_{yi}\beta_{yj} \left[(b_{2i}b_{2j} - 2b_{3i}b_{2j}\eta_{xi} + 4b_{3i}b_{3j}\eta_{xi}\eta_{xj}) e^{i2(\mu_{yi}-\mu_{yj})} + 2b_{3i}b_{2j}\eta_{xi} e^{-i2(\mu_{yi}-\mu_{yj})} \right] \\ & - \frac{i}{8} \sqrt{\beta_{xi}\beta_{xj}\beta_{yj}\eta_{xi}} (b_{3i}\eta_{xi} - b_{2i}) b_{3j} \left[e^{i(\mu_{xi}-\mu_{xj})} - e^{-i(\mu_{xi}-\mu_{xj})} \right] \Big\}, \end{aligned} \tag{A.49}$$

$$\begin{aligned} h_{00202} = \sum \Big\{ & \frac{i}{16} \beta_{yi}\beta_{yj} \left[(b_{2i}b_{2j} - 2b_{3i}b_{2j}\eta_{xi} + 4b_{3i}b_{3j}\eta_{xi}\eta_{xj}) e^{i2\mu_{yi}} + 2b_{3i}b_{2j}\eta_{xi} e^{i2\mu_{yj}} \right] \\ & - \frac{i}{16} \sqrt{\beta_{xi}\beta_{xj}\beta_{yj}\eta_{xi}} (b_{3i}\eta_{xi} - b_{2i}) b_{3j} \left[e^{i(\mu_{xi}-\mu_{xj}+2\mu_{yj})} - e^{-i(\mu_{xi}-\mu_{xj}-2\mu_{yj})} \right] \Big\}, \end{aligned} \tag{A.50}$$

$$\begin{aligned} h_{10003} = \sum \Big\{ & \frac{i}{4} b_{3i} b_{2j} \beta_{xi} \sqrt{\beta_{xj}\eta_{xi}\eta_{xj}} \left[e^{i\mu_{xj}} - e^{i(2\mu_{xi}-\mu_{xj})} \right] \\ & + \frac{i}{8} \sqrt{\beta_{xi}\beta_{xj}\eta_{xi}} \left[b_{2i}b_{2j} - b_{3i}\eta_{xi}(b_{2j} - 2b_{3j}\eta_{xj}) \right] \left[e^{i\mu_{xi}} - e^{-i(\mu_{xi}-2\mu_{xj})} \right] \Big\}, \end{aligned} \tag{A.51}$$

$$h_{00103} = 0, \tag{A.52}$$

$$h_{00004} = \sum \frac{i}{4}\sqrt{\beta_{xi}\beta_{xj}\eta_{xi}\eta_{xj}}\Big\{\big[b_{2i}b_{2j} - b_{3i}\eta_{xi}(b_{2j} - b_{3j}\eta_{xj})\big]e^{i(\mu_{xi}-\mu_{xj})} + b_{3i}b_{2j}\eta_{xi}e^{-i(\mu_{xi}-\mu_{xj})}\Big\}. \tag{A.53}$$

The coefficients $b_2 = K_1 L$ and $b_3 = K_2(L/2)$, where $K_1$and K_2 are quadrupole and sextupole strength used in ELEGANT and MAD, and L is the magnet length.

A.2 Piwinski's formula for Touschek lifetime

From Piwinski's formula [48], Touschek lifetime can be written in simple form as

$$\frac{1}{T_l} = \langle \frac{R}{N_0} \rangle, \tag{A.54}$$

where R is the total of scattering occur and N_0 is the initial total number of particles in a bunch. The larger scattering rate the lower lifetime can be. The total scattering is given by

$$R = \frac{r_p^2 c\beta_x\beta_y\sigma_h N_b^2}{8\sqrt{\pi}\beta^2\gamma^4\sigma_{x\beta}^2\sigma_{y\beta}\sigma_s\sigma_p} F(\tau_m, B_1, B_2), \tag{A.55}$$

with

$$F = \int_{\tau_m}^{\infty} e^{-B_1\tau} I_0(B_2\tau) \frac{\sqrt{\tau}\mathrm{d}\tau}{\sqrt{1+\tau}} ((2+\frac{1}{\tau})^2(\frac{\tau/\tau_m}{1+\tau} - 1) + 1 - \frac{\sqrt{1+\tau}}{\sqrt{\tau/\tau_m}} - \frac{4\tau+1}{2\tau^2}\ln\frac{\tau/\tau_m}{1+\tau}), \tag{A.56}$$

$$B_1 = \frac{1}{2\beta^2\gamma^2}\left(\frac{\beta_x^2}{\sigma_{x\beta}^2} - \frac{\beta_x^2\sigma_h^2\tilde{\eta}_x^2}{\sigma_{x\beta}^4} + \frac{\beta_y^2}{\sigma_{y\beta}^2} - \frac{\beta_y^2\sigma_h^2\tilde{\eta}_y^2}{\sigma_{y\beta}^4}\right), \tag{A.57}$$

$$B_2 = \sqrt{B_1^2 - \frac{\beta_x^2\beta_y^2\sigma_h^2}{\beta^4\gamma^4\sigma_{x\beta}^4\sigma_{y\beta}^4\sigma_p^2}(\sigma_x^2\sigma_y^2 - \sigma_p^4\eta_x^2\eta_y^2)}, \tag{A.58}$$

$$\tau_m = \beta^2\delta_m^2 = \beta^2\left(\frac{\Delta p_m}{p}\right)^2, \tag{A.59}$$

$$\sigma_h = \frac{\sigma_{x\beta}\sigma_{y\beta}\sigma_p}{\sqrt{\tilde{\sigma}_x^2\sigma_{y\beta}^2 + \tilde{\sigma}_y^2\sigma_{x\beta}^2 - \sigma_{x\beta}^2\sigma_{y\beta}^2}}, \tag{A.60}$$

$$\tilde{\eta}_{x,y} = \alpha_{x,y}\eta_{x,y} + \beta_{x,y}\eta'_{x,y}, \tag{A.61}$$

$$\tilde{\sigma}_{x,y}^2 = \sigma_{x\beta,y\beta}^2 + \sigma_p^2(\eta_{x,y}^2 + \tilde{\eta}_{x,y}^2), \tag{A.62}$$

where r_c is the classical particle radius, $\beta_{x,y}, \alpha_{x,y}, \eta_{x,y}$ and $\eta'_{x,y}$ are the optics functions, N_b is the number of particles per bunch, $\sigma_{x,y,s}$ are the rms beam size in horizontal, vertical and longitudinal plane respectively, σ_p is the energy spread, β and γ are the Lorentz factor and $\sigma_{x\beta,y\beta}$ are the beam size without momentum spread.